A Probabilistic Model for Capacity in Wireless Multihop Networks

A Probabilistic Model for Capacity in Wireless Multihop Networks

Patrick Stuedi and Gustavo Alonso

Swiss Federal Institute of Technology (ETHZ)
Departement of Computer Science
8092, ETH-Zentrum, Switzerland
{stuedip, alonso}@inf.ethz.ch

Abstract— **Capacity is an important property for QoS support in Mobile Ad Hoc Networks (MANETs) and has recently attracted considerable attention in research. However, most approaches rely on simplified models (infinite network, isotropic radio propagation, unidirectional links, perfect scheduling, etc.) and provide only asymptotic bounds or integer linear programming equations. In this paper we take a probabilistic approach and model capacity as a random variable that depends on node distribution, communication pattern, radio propagation and channel assignment. Expected values for the random variable at a given point within the parameter space are then computed using Monte-Carlo simulation. The modularity of the approach allows for capacity analysis under more realistic network models. We demonstrate the potential of such a model by showing that for acknowledgement-based networks throughput capacity increases in the presence of shadowing, even above the critical node density.**

I. INTRODUCTION

Capacity is typically studied by choosing a network model that facilitates analytical treatment. Most existing work assumes a network to have n nodes distributed within a certain area and defines a transmission between two nodes to be successful if its signal-to-noise ratio is bigger than a given threshold. In [8], capacity is then studied asymptotically for an increasing node density. It is shown that the throughput capacity $\lambda(n)$ for a network of n nodes within an area of $[0, 1]^2$ is in the order of $\Theta(W/\sqrt{nlogn})$. This result was extended for models including variable transmission power [7] and bound attenuation functions [6]. While asymptotic bounds certainly indicate the generic behavior of ad hoc networks for large n, they do not give any information on concrete throughput capacity in small networks. Recently, there has been some effort to tackle this problem [3], [5], [16] using integer linear programming (*ILP*). However, *ILP* makes it very difficult to model physical network properties such as realistic signal propagation, link asymmetry or interference. As a consequence most of these studies are based on a simplified network model. For instance it is common to predict the received power as a deterministic function of distance, thereby representing the communication range as an ideal circle. In reality, the received power at a certain distance is a random variable due to fading effects. Effects of shadowed radio propagation on capacity have also been analyzed [18] but without considering multihop

networks. In such networks any variation in the signal pattern impacts the perceived interference at a given node. Non-deterministic variation of signal power may further lead to link asymmetry. This behavior was measured experimentally in [1]. IEEE 802.11, the MAC protocol often mentioned in combination with ad hoc networks, allows for data transmission only if there exists a bi-directional connection between the two communicating nodes since data packets need to be acknowledged by the receiving node. Effects of asymmetric links on higher network layers were investigated in [17].

In this paper we explore capacity in multihop wireless networks by relaxing some of these assumptions. We do so by developing a probabilistic model of throughput capacity as a random variable depending on node topology, communication pattern, interference model, signal propagation and channel assignment. Expected values of the random variable are then computed using a Monte-Carlo estimator. The advantage of our approach lies in its decoupling from specific network characteristics, a feature that allows us to investigate throughput capacity under specific network topologies and communication patterns, including random ones. In particular, the model may serve as a basis for testing and verifying channel assignment and routing strategies with respect to throughput capacity. This is of special interest since the interaction between routing and channel assignment is rather complex and difficult to treat analytically. Furthermore, given a specific topology and a channel assignment strategy, the model predicts throughput capacity for the various communication flows. For instance in a sensor network one might be interested in an estimate of the throughput capacity when all the sensors transmit data towards a common sink. Moreover, effects of different models for signal propagation and interference can also be analyzed using the proposed model.

The rest of the paper is structured as follows: Sections II and III describe the model. In section IV we validate the model with respect to small static networks. Coloring networks with different radio thresholds is discussed in section V. The following section aims at verifying the model under more realistic network configurations – including random networks – by comparing the prediction to results obtained through ns-2 simulations. Section VII shows the flexibility of the proposed

probabilistic approach by means of two use cases: randomized radio propagation and variable interference range. The paper concludes finally with section VIII.

II. NETWORK MODEL

In a first step, we want to turn physical properties of wireless multihop networks, like node locations or perceived signal strengths, into a so called *schedule graph* $G(\mathcal{N}, E)$, where $\mathcal{N}$ is the set of nodes and E corresponds to the set of links between these nodes (a link between two nodes indicating the two nodes can communicate with each other). The idea is to – later on – let the throughput capacity computation be exclusively based on the graph. In this section, we first define some common properties in order to then gradually develop the graph representation by assigning four sets $\mathcal{I}_i \supseteq \mathcal{D}_i \supseteq \mathcal{U}_i \supseteq \mathcal{V}_i$ of nodes to each node n_i, with $\mathcal{I}_i \supseteq \mathcal{N}$. Nodes within the particular sets correspond to the different forms of interaction nodes can have, such as interfering, decoding, unidirectional communication and bidirectional communication:

- $\mathcal{I}_i$: Set of nodes that interfere with node n_i
- $\mathcal{D}_i$: Set of nodes that can be correctly decoded at node n_i if there is no interference
- $\mathcal{U}_i$: Set of nodes that can be decoded at node n_i even if there is interference
- $\mathcal{V}_i$: Set of nodes that can be considered as neighbors of n_i

In principle, the network – as we are going to present it – is parameterized by the following four properties: A node distribution $\delta_\mathcal{A}$, a signal propagation φ, a channel assignment ψ and an interference model κ. We consider a set $\mathcal{N} = \{n_0, n_1..., n_{N-1}\}$ of N nodes, distributed according to some probability density function $\delta_\mathcal{A} : (x, y) \longrightarrow [0..1]$, defined over an area $\mathcal{A}$. Further assume a channel assignment $\psi : \mathcal{N} \longrightarrow \Gamma$ for a common channel Γ, such that every node n_i has one subchannel $n_i^\Gamma \in \Gamma$ assigned. We therefore say the common channel Γ is divided into T subchannels, $\Gamma = \{\Gamma^0, \Gamma^1..., \Gamma^T\}$, where typically $T < N$. The nodes are not allowed to transmit data in any other than their subchannel. Receiving is possible from all the subchannels. For the sake of simplicity we use the word subchannel interchangeably for the set of all nodes transmitting data within that specific subchannel, or $\Gamma^\alpha = \{n_i | n_i^\Gamma = \Gamma^\alpha\}$.

A. Interferers $\mathcal{I}_i$

A node n_i is assumed to transmit with power p_i^t. For a certain signal propagation $\vartheta : \mathbb{R} \longrightarrow \mathbb{R}$, the received signal strength $p^r(d)$ at distance d is computed as $p_i^t \cdot \vartheta(d)$. Therefore, the signal power $p_{j,i}^r$ perceived at node n_i due to a transmission of node n_j is determined by $p_i^t \cdot \vartheta(|x_j - x_i|)$, where x_* are the coordinates of node i. In the simplest case ϑ is a direct function of the distance. The path loss radio propagation model, for example, defines $\vartheta_{pl}(d) = d^{-\rho}$ for some path loss exponent ρ. A more sophisticated model is the log normal shadowing radio propagation [12]:

$$\vartheta_{sh}(d) \sim \frac{1}{10^{\rho \log_{10}(d) - X/10}} \quad (1)$$

where X is a gaussian random variable with zero mean and standard deviation σ and ρ is the aforementioned path loss exponent. In case of σ equal 0, there is no random effect and $\vartheta_{sh} \sim \vartheta_{pl}$.

A node $n_j \neq n_i$ belongs to the set of interferers $\mathcal{I}_i$ of node n_i in case the signal power $p_{j,i}^r$ perceived at node n_i due to a transmission of node n_j exceeds a certain interference threshold β_I:

$$\mathcal{I}_i = \{n_j \mid n_j \neq n_i \ and \ p_{j,i}^r > \beta_I\}. \quad (2)$$

B. Decodables $\mathcal{D}_i$

Similar to $\mathcal{I}_i$, the set of decodables $\mathcal{D}_i$ of node n_i is defined as

$$\mathcal{D}_i = \{n_j \mid n_j \neq n_i \ and \ p_{j,i}^r > \beta_D\}, \quad (3)$$

with $\beta_D > \beta_I$. We call β_D the decoding threshold. Distinguishing between $\mathcal{D}_i$ and $\mathcal{I}_i$ takes into account that radio receivers are typically much more sensitive to interference than to signal decoding.

C. Senders $\mathcal{S}_i$

Whether $n_j \in \mathcal{U}_i$, meaning n_i can decode the signal of node in spite of interference is decided by an interference model $\kappa : \mathbb{R} \times \mathbb{R} \longrightarrow \{0, 1\}$ with

$$\kappa(p_{j,i}^r, \Lambda_i^\alpha) = \begin{cases} 1 & p_{j,i}^r \text{ can be decoded under noise } \Lambda_i^\alpha \\ 0 & p_{j,i}^r \text{ cannot be decoded} \end{cases} \quad (4)$$

.

Here Λ_i^α denotes the noise perceived at n_i while listening to the subchannel $n_j^\Gamma = \Gamma^\alpha$ assigned to node n_j. More formally

$$\Lambda_i^\alpha = \begin{cases} \sum_{\substack{k \in \Gamma^\alpha \\ k \neq i}} p_{k,i}^r & \text{if } n_i^\Gamma \neq \Gamma^\alpha \\ \infty & \text{otherwise} \end{cases} \quad (5)$$

.

A node $n_j \in \mathcal{D}_i$ is part of $\mathcal{U}_i$ if and only if $\kappa(p_{j,i}^r, \Lambda_i^a) = 1$, i.e:

$$\mathcal{U}_i = \{n_j | j \neq i \ \wedge \ e(p_{j,i}, \Lambda_i^\alpha) = 1\} \quad (6)$$

The most common interference model is based on the so called signal-to-noise ratio:

$$SNR_{j,i} = \frac{p_{j,i}^r}{W_0 + \Lambda_i^\alpha} \quad (7)$$

.

This leads to an interference model as follows

$$\kappa_{snr}(p_{j,i}^r, \Lambda_i^a) = 1 \iff SNR_{j,i} > \beta_{snr} \quad (8)$$

,

for a threshold β_{snr}. Of course it must be given that

$$\frac{p^r_{j,i}}{N_0} \geq \beta_{snr} \iff p^r_{j,i} \geq \beta_I, \qquad (9)$$

where N_0 denotes the ground noise.

D. Neighbors $\mathcal{N}_i$

In our model we particularly want to account for acknowledgement based medium access protocols. We therefore define $\mathcal{V}_i$, the set of all neighbors of n_i as follows:

$$\mathcal{V}_i = \{n_j | j \neq i \land n_j \in \mathcal{U}_i \land n_i \in \mathcal{D}_j \} \qquad (10)$$

This set includes all nodes n_j that are senders for n_i (i.e., can transmit and their transmission is properly received by n_i) and can receive the acknowledgement sent back by n_i. Note that equation 11 models the acknowledgment itself as an infinite small packet not occupying the medium. Based on the definition of neighbors, we finally introduce the notion of a *schedule graph*. A *schedule graph* is a directed graph $G_T(\mathcal{N}, E)$, where T denotes the number of subchannels in Γ, $\mathcal{N}$ corresponds to the set of nodes and E is the set of edges defined as

$$E = \{(n_j, n_i) | n_i \in \mathcal{N} \land n_j \in \mathcal{V}_i\}. \qquad (11)$$

From the definition of a *schedule graph* $G_T(\mathcal{N}, E)$ it directly follows that a path between two nodes n_u, n_v states that there is a sequence of nodes $\{n_u, n_{u+1}, ...n_v\}$ as well as schedule of time slots $\{n_u^\Gamma, n_{u+1}^\Gamma, ...\}$ such that node n_u is able to consecutively transmit data at a rate $\xi > 0$.

III. THROUGHPUT CAPACITY

Throughout this section an ad hoc network is represented by its corresponding *schedule graph* $G_T(\mathcal{N}, E)$. Throughput capacity is defined over a set Υ_m of measured communication pairs which is a subset of all existing communication Υ pairs in an ad hoc network:

$$\Upsilon_m \subseteq \Upsilon \subseteq \{(n_i, n_j) | \forall i, \forall j, i \neq j \land n_i \in \mathcal{N} \land n_j \in \mathcal{N}\}. \quad (12)$$

More precisely, we say that a *schedule graph* $G_T(\mathcal{N}, E)$ with a communication pattern Υ has a throughput capacity with respect to Υ_m of λ_m if on average a communication pair $v \in \Upsilon_m$ can expect an end-to-end throughput of λ_m bits per second. In most cases we have $\Upsilon_m = \Upsilon$.

Important to the computation of throughput capacity is the routing $\eta : (n_j, n_i) \longrightarrow \{n_u, n_v, ..n_w\}$. We define

$$\Pi_{j,i} = \eta((n_j, n_i)), \quad with (n_j, n_i) \in \Upsilon_m \qquad (13)$$

to be the sequence of nodes included in the path from n_j to n_i, excluding n_i.

We now want to provide an estimator λ_m^* for λ_m, so that $\lambda_m^* \approx \lambda_m$. The approach we follow is of a probabilistic nature. Basically, we model throughput capacity as a random variable ζ and compute its expected value, with $E[\zeta] = \lambda^*$. In order to show how ζ is defined we need some helper variables. We

assume $Sched_{j,i}$ to be a random variable indicating whether a schedule between node n_j and n_i exists. This is equal to the question of whether there is a path between j and i within the *schedule graph* $G_T(\mathcal{N}, E)$:

$$Sched_{j,i} = \begin{cases} 1 & \text{if there is a path between } n_j \text{ and } n_i \\ 0 & \text{otherwise.} \end{cases} \qquad (14)$$

Based on the notion of $\Pi_{j,i}$ we define Π^Υ as follows:

$$\Pi^\Upsilon = \{\Pi_{j,i} | (j, i) \in \Upsilon\}. \qquad (15)$$

The random variable $B_{j,i}$ is then defined as

$$B_{j,i} = \max_{n \in \Pi_{j,i}} \{ \sum_{P_{u,v} \in (\Pi \backslash \Pi_{j,i})} F(n, \Pi_{u,v})\}, \qquad (16)$$

where F is the membership function,

$$F(n, \Pi_{u,v}) = \begin{cases} 1 & \text{if } n \in \Pi_{u,v} \\ 0 & \text{otherwise.} \end{cases} \qquad (17)$$

$B_{j,i}$ takes into account to what extent the path between n_j and n_i is shared with other ongoing communication pairs.

Based on the definition of $Sched_{j,i}$ and $B_{j,i}$ we now claim the achievable throughput $\zeta_{j,i}$ in a *schedule graph* $G_T(\mathcal{N}, E)$ to be modelled by the random variable

$$\zeta_{j,i} = \frac{W \times Sched_{j,i}}{B_{j,i} \times T}, \qquad (18)$$

where W is the maximum transmission rate equal to all nodes. With respect to a measurement set Υ_m and for a uniformly chosen communication pair $(j, i) \in \Upsilon_m$ we can further state that

$$\zeta^m = \frac{1}{|\Upsilon_m|} \sum_{(u,v) \in \Upsilon_m} \zeta_{u,v}, = \frac{W}{|\Upsilon_m| \times T} \sum_{(u,v) \in \Upsilon_m} \frac{Sched_{j,i}}{B_{j,i}}, \qquad (19)$$

and therefore

$$\lambda_m \approx E[\zeta^m] = \frac{W}{|\Upsilon_m|} \sum_{(u,v) \in \Upsilon_m} E[\frac{Sched_{j,i}}{T \times B_{j,i}}] = W \times E[\Omega] \qquad (20)$$

where $\Omega = Sched_{j,i} \backslash T \backslash B_{j,i}$ for any $(j, i) \in \Upsilon_m$.

IV. APPROXIMATING CAPACITY IN STATIC NETWORKS

As an example of how the model operates and as an intuitive validation, in this section we compute λ^* for two simple, static scenarios. Static in the sense that the network topology as well as the communication pattern is fixed. We will consecutively derive λ^* by going through the basic steps of section II and III. For reasons of simplicity assume $\beta_I = \beta_D$. Therefore, the set of interferers $\mathcal{I}_i$ equals the set of decodables $\mathcal{D}_i$ for all nodes i.

The simplest network topology we want to discuss consists of three nodes being equally far apart from each other, as shown in Figure 1. A dashed line between two nodes j and i

T	n_i^Γ	$\mathcal{U}$	Υ	$Sched_{j,i}$	$B_{j,i}$	λ^*
1	-	$\emptyset$	-	0	-	0
2	A: 0	$\mathcal{U}_A = \{B\}$	(A,B)	$Sched_{A,B} = 0$	0	1/6
	B: 1	$\mathcal{U}_B = \emptyset$	(B,C)	$Sched_{B,C} = 1$	1	
	C: 0	$\mathcal{U}_C = \{B\}$	(C,A)	$Sched_{C,A} = 0$	0	
			(A,C)	$Sched_{A,C} = 0$	0	1/6
			(B,A)	$Sched_{B,A} = 1$	2	
			(B,C)	$Sched_{B,C} = 1$	2	
3	A: 0	$\mathcal{U}_A = \{B,C\}$	(A,B)	$Sched_{A,B} = 1$	1	1/3
	B: 1	$\mathcal{U}_B = \{A,C\}$	(B,C)	$Sched_{B,C} = 1$	1	
	C: 2	$\mathcal{U}_C = \{A,B\}$	(C,A)	$Sched_{C,A} = 1$	1	

TABLE I

STATES FOR THE TRIANGLE SCENARIO

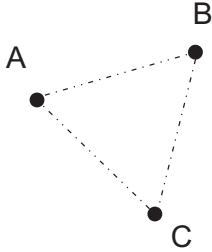| T	n_i^Γ	$\mathcal{U}$	Υ	$Sched_{j,i}$	$B_{j,i}$	λ^*
1	-	$\emptyset$	-	0	-	0
2	A: 0	$\mathcal{U}_A = \{B\}$	(A,B)	$Sched_{A,B} = 1$	1	1/6
	B: 1	$\mathcal{U}_B = \{A\}$	(B,C)	$Sched_{B,C} = 0$	0	
	C: 1	$\mathcal{U}_C = \emptyset$	(C,A)	$Sched_{C,A} = 0$	0	
	A: 0	$\mathcal{U}_A = \{B\}$	(A,B)	$Sched_{A,B} = 1$	1	1/3
	B: 1	$\mathcal{U}_B = \emptyset$	(B,A)	$Sched_{B,A} = 1$	1	
	C: 0	$\mathcal{U}_C = \{A\}$	(C,A)	$Sched_{C,A} = 0$	-	
3	A: 0	$\mathcal{U}_A = \{B,C\}$	(A,B)	$Sched_{A,B} = 1$	1	5/18
	B: 1	$\mathcal{U}_B = \{A,C\}$	(B,A)	$Sched_{B,C} = 1$	1	
	C: 2	$\mathcal{U}_C = \{A,B\}$	(C,A)	$Sched_{B,A} = 1$	2	
			(A,B)	$Sched_{A,B} = 1$	1	1/3
			(B,A)	$Sched_{B,A} = 1$	1	
			(C,B)	$Sched_{C,B} = 1$	1	

TABLE II

STATES FOR THE CHAIN SCENARIO

Fig. 1.   A simple triangle scenario

assignments in Table I. Assigning the same channel ($T = 1$) to all nodes leads to $\mathcal{U}_i = \emptyset$ for all nodes and therefore to $E = \emptyset$, $Sched_{j,i} = 0$, $\zeta_{j,i} = 0$, $\lambda^* = 0$. If we assign two channels ($T = 2$) to the three nodes, only two directed links can be established (among the potential 6). In the case of $\Upsilon = \Upsilon_m = \{(A,B), (B,C), (C,A)\}$ as the communication pattern (see Table I), λ^* is $0 + 1/6 + 0 = 1/6$, according to equation 19 . If we have $\Upsilon_m = \{(A,B), (B,A), (B,C)\}$, λ^* equals $0 + 1/12 + 1/12 = 1/6$. Using 3 channels ($T = 3$) leads to a fully connected graph. λ^* is then $1/9 + 1/9 + 1/9 = 1/3$.

indicates $n_j \in \mathcal{I}_i$, $n_j \in \mathcal{D}_i$, $n_i \in \mathcal{I}_j$, $n_i \in \mathcal{D}_j$. Let us further assume a very simple interference model:

$$\kappa_{ns2}(p_{j,i}^r, \Lambda_i^a) = \begin{cases} 1 & \text{if } p_{j,i}^r > \Lambda_i^a \\ 0 & \text{otherwise} \end{cases} \qquad (21)$$

We will use κ_{ns2} later on in section VI when comparing the model's estimate with results taken from ns-2 simulations.

In order to transform the topology information into a graph G_T we need to assign channels to the nodes. Searching for the optimal channel assignment refers to the class of vertex coloring problems, which is in most cases NP-hard [9]. However, for the topology in Figure 1 there are only three possible ways to assign the channels to the nodes. We keep track of all states and sets of the network model for each of the three channel
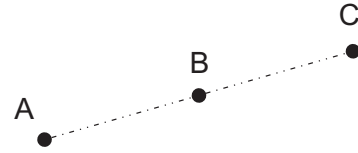

Fig. 2.   A simple chain scenario

The situation is slightly different in Figure 2 since node B acts as a router and some of its bandwidth is consumed by traffic sent from A to C. As shown in Table II, there are two ways to assign two colors to the three nodes. Depending on the channel assignment and the communication pattern, a 2-channel-solution might even perform better on average than using 3 channels.
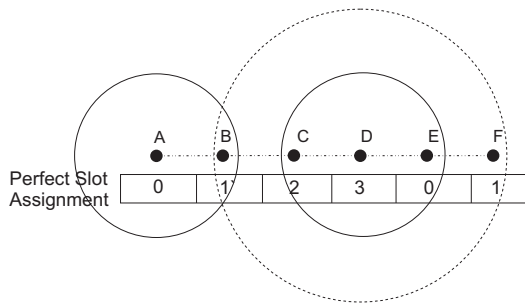
Fig. 3. Channel assignment with variable interference

Fig. 4. Coloring the transmission and interference graph

V. COLORING MULTI-LAYER-GRAPHS

As previously mentioned, channel assignment refers to the problem of graph coloring and is known to be NP-hard in most cases. Given a graph $G(V, E)$, classical graph coloring aims at coloring V with the minimum number of colors such that for each edge $(i, j) \in E$, vertexes i and j have different colors. The more specific problem of coloring multihop wireless networks in order to achieve an entirely collision-free schedule is also known as distance-2-coloring, [9], [11]. Such a coloring assigns different colors to any pair of nodes between which there is a path of length at most 2. This distance-2-coloring problem on a graph G is equivalent to the standard minimum vertex coloring [11] problem on G^2, where G^2 has the same vertex set as G and there is an edge between two vertices of G^2 if and only if there is a path of length at most 2 between the vertices in G. Unfortunately, solving the distance-2-coloring problem does not provide a collision-free schedule in multihop wireless networks if the transmission range and the interference range differ. In fact today's radio receivers are much more sensitive to interference than to signal decoding. In our model these two thresholds are given by β_I and β_D. Figure 3 illustrates the effect of different thresholds on the channel assignment by means of a chain topology. It is assumed that $\beta_I > 2 \times \beta_D$, an assumption that can be found, e.g., in the network simulator ns-2 [15] for example. As a consequence, node D's packet transmission in Figure 3 will interfere with packets sent from A to B. A perfect channel assignment for such a graph would require 4 channels. A pure distance-2-coloring would produce either 5 or 3 channels instead, depending on whether the algorithm operates on the interference graph or on the transmission graph. Figure 4 illustrates this point. Edges of the transmission graph are shown by dashed lines, referring to the set $\mathcal{U}$ in our model. The interference graph extends the transmission graph by additionally including edges drawn with solid lines ($\mathcal{I}$ in our model). Given a simple interference model like the one described in equation 25, applying distance-2-coloring to the transmission graph results in broken links and therefore potentially prohibits a schedule (Equation 14). On the other hand, using distance-2-coloring on the interference graph does not produce the minimum number of channels since it assigns different channels to nodes A and E. Indeed, the transmission
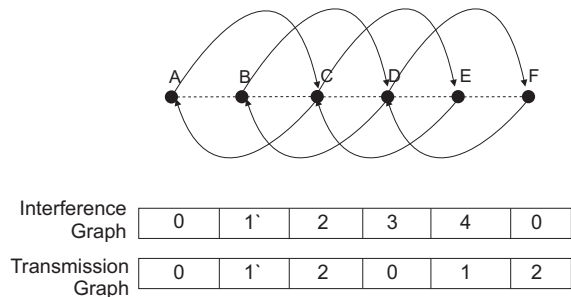
of both nodes A and E are interfering at node C and one may wish all the nodes $A - E$ to transmit in different channels. However, far more important is that transmissions between C and its direct neighbors do not interfere with A and E. This can easily be achieved by assigning a minimum of 4 channels as shown in Figure 3.

Finding generic algorithms or good approximations for a minimum channel assignment in the described manner is not within the scope of this paper. Rather, we use two simplified channel assignment algorithms for the rest of the paper: *GreedyM* and *RandomNode*. The *GreedyM* assignment basically extends the classical greedy algorithm to take the multi-layer aspect into account. It takes each vertex in turn and tries to color the vertex with one of the colors used so far, prohibiting neighboring nodes to transmit in the same channel as interfering nodes. In other words, it tries to add the vertex to one of the existing color classes. If this is not possible due to some interferers already having the same channel assigned, then a new color class is created and the vertex is assigned the color of that class. See Algorithm 1 for a detailed description. The *RandomNode* (Algorithm 2) channel assignment on the other hand just assigns a set of of channels in a round robin manner to the nodes. At each round a node is picked on a random basis. In the following sections we will see how channel assignments affect capacity.

VI. PREDICTING CAPACITY OF 802.11 AD HOC NETWORKS

After having introduced the model by means of small static examples, we now proceed to see whether we can use the model to predict throughput capacity in 802.11 ad hoc networks, including random topologies. Remember that the model predicts throughput capacity as $W \cdot E[\Omega]$ where Ω denotes the random variable composition $Sched_{j,i}/T/B_{j,i}$ for any $(j, i) \in \Upsilon_m$. One could compute $E[\Omega]$ given the common probability density $f_{sched,T,B}(s, t, b)$ for the random variables $Sched, T$ and B. However, finding the density function $f_{sched,T,B}$ is not trivial. In fact the problem can be viewed as an extension to the traditional connectivity problem where one tries to find the probability of whether a given node distribution and transmission range results in a connected network. In this paper we do not pursue an analytical treatment of $E[\Omega]$ but

Algorithm 1 GreedyM

```
 1: INPUT 𝒩 := {n₀...n_{N-1}};
 2: for all nᵢ ∈ 𝒩 do
 3:     𝒬 := {Γⁱ..Γ^{N-1}};
 4:     if nᵢ^Γ ∈ Γ then
 5:         𝒬 := 𝒬 \ nᵢ^Γ;
 6:     end if
 7:     for all nⱼ ∈ ℐᵢ do
 8:         if nⱼ^Γ ∈ Γ then
 9:             𝒬 := 𝒬 \ nⱼ^Γ;
10:         end if
11:     end for
12:     if nᵢ^Γ ∉ Γ then
13:         nᵢ^Γ := min {Γ^α ∈ Γ};
14:         𝒬 := 𝒬 \ nᵢ^Γ;
15:     end if
16:     for all nⱼ ∈ 𝒟ᵢ do
17:         if nⱼ^Γ ∉ Γ then
18:             nⱼ^Γ := min {Γ^α ∈ Γ};
19:             𝒬 := 𝒬 \ nⱼ^Γ;
20:         end if
21:     end for
22: end for
```

Algorithm 2 RandomNode$_X$

```
 1: INPUT 𝒩 := {n₀...n_{N-1}};
 2: MAXCHANNEL := X;
 3: 𝒪 := 𝒩;
 4: i := 0;
 5: α := 0;
 6: Γ := ∅;
 7: while i ≤ |𝒪| do
 8:     n := ANY{n ∈ 𝒪};
 9:     𝒪 := 𝒪 \ n;
10:     n^Γ = Γ^α;
11:     Γ := Γ ∪ Γ^α;
12:     α := (α + 1) MOD MAXCHANNEL;
13: end while
```

rather use a Monte-Carlo estimator:

$$E[\Omega] \approx \frac{1}{K} \sum_{i=1}^{K} \Omega_i. \tag{22}$$

Or in other words, we approximately compute the expected value of Ω for a given set of parameters by averaging over K realizations of the underlying random network.

In order to verify the quality of our predictions we compare the computed estimate to ns-2 simulation results. Throughout section VI we use the interference model as described in equation 25. The model serves as a very basic approximation of the ns-2 interference model. To avoid mixing up capacity measurements with routing issues, packets within ns-2 simulations are forwarded using pre-computed shortest path routes. In all setups, the thresholds β_I and β_D are set such that $\beta_i = 5/11 \times \beta_D$. This corresponds to the default ns-2 setting. Furthermore β_D is configured such that it produces a transmission range of 250 meters. We have set the MAC data rate in ns-2 to 1Mbit since operating 802.11 at higher rates results in drastically reduced efficiency and makes the measurements difficult to compare as the relative time spent on the per-packet overhead dominates. This is due to the 802.11

preamble which must be of a fixed length because it is used by the hardware for bit synchronization.
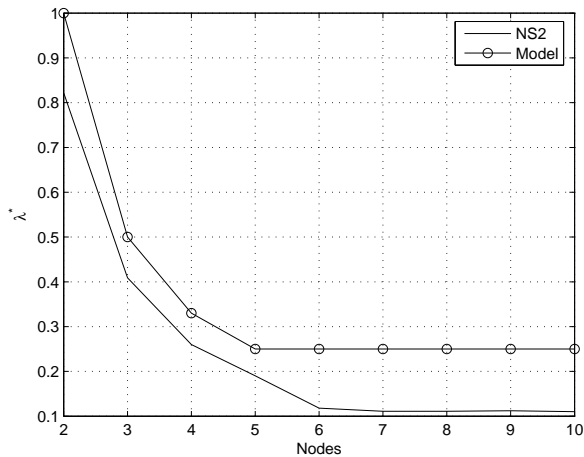
A. Chain

In a first comparison we look at the the simplest possible case of a chain of n nodes. Each node is 200 meters away from its neighbor. The first node acts as a source of data traffic, the last node is the traffic sink. Data is sent as fast as the MAC allows. Regarding the model, we use $GreedyM$ as the channel assignment algorithm. It can easily be verified that $GreedyM$ finds a minimal channel assignment for a chain of any size. Since there are no random components involved, λ^* is a direct function of the channels needed, and computes to $1/4$ as the chain grows. From Figure 5a we see that the prediction overestimates the real measured throughput, especially when the chain becomes large. This is due to the overhead of headers, RTS, CTS and ACK packets but also because in reality nodes fail to achieve an optimal schedule. The results obtained with our model match those presented in [10], where the authors discuss throughput capacity measurements taken from ns-2 simulations with respect to theoretical upper bounds.

As a first step towards more realistic scenarios, we now investigate random communication patterns in chain topologies. For this purpose, we assign a random destination $d(n_i) \in \mathcal{N} \backslash n_i$ to every node $n_i \in \mathcal{N}$. Figure 5b shows a quite good match between λ^* based on perfect channel assignment (using $GreedyM$) and the measurements obtained with ns-2. This is not too surprising since we know from Figure 5a that λ^* matches quite well the simulation results if the path length is short. And the average path length under random communication is expected to be far below the maximum value of $n - 1$, for a chain of length n. Furthermore overlapping communication paths reduce capacity due to the forwarding load induced to the nodes, especially if the chain becomes large. By taking the effect of forwarding load into account, our model is able to quite accurately estimate the available capacity under random communication.

B. Grid

While the $GreedyM$ algorithm leads to a conflict-free channel assignment in a chain topology, it does not in a grid topology. This is illustrated in Figure 6a. The grey zone represents the interference area of the node located at the upper left hand corner. Similarly, the non-shadowed region denotes the interference area of the second node. The lines starting at the first two nodes refer to the stepwise channel assignment performed by $GreedyM$. The algorithm finally produces a conflict when the two neighbors indicated by a surrounding circle are assigned the same channel. In order to achieve a conflict-free schedule in a grid, one would have to assign at least 16 channels to the nodes[1], as shown in Figure 6b. However, rather than asking for a conflict-free schedule, the more important question would be how to achieve a maximum throughput capacity λ^*. Interestingly, a conflict-free schedule

---
[1]Derives directly from the optimal 4-channel assignment in the chain
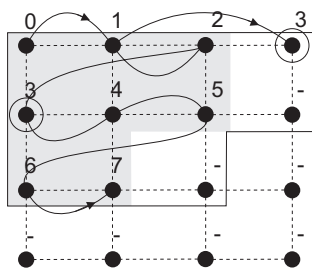
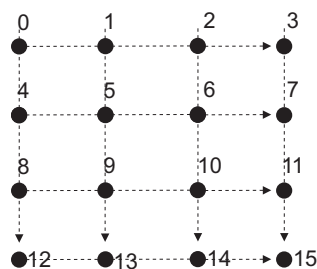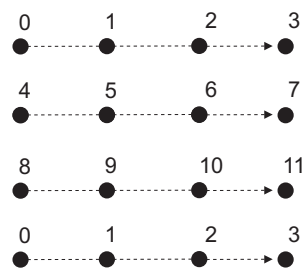(a) Single end-to-end flow
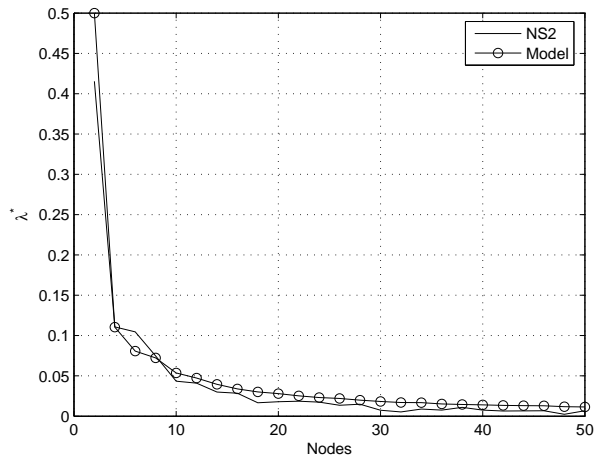
(b) Random communication

Fig. 5.   Chain Topology

(a) GreedyM Algorithm

(b) Cross Traffic

(c) Horizontal Traffic

Fig. 6.   Channel assignment in the grid

does not necessarily lead to a maximum throughput capacity. This can easily be verified in Figure 6c, a scenario in which data traffic is only routed horizontally. Since there is, e.g., no communication going on between nodes in the first chain and their direct neighbors in the second chain, it is no problem to assign the same channels to both the first and the last chain in the grid. Such an assignment strategy only uses 12 channels, rather than the maximum of 16 for a conflict-free schedule and therefore achieves a higher throughput capacity given the communication pattern of Figure 6c. Or in a more generic way, knowledge of the communication and routing pattern that takes place in the network is crucial to achieve a minimum channel assignment. Our model may serve as a basis for further research on the complex interaction between routing and channel assignment with regard to throughput maximization. The trade-off between routing and channel assignment has also been taken into account by [2], [13] where the authors propose a hybrid routing/scheduling algorithm to gradually improve throughput capacity.

After having described the routing-scheduling trade-off and the non-optimality of $GreedyM$ in the grid topology, we now compare the throughput estimate λ^* with ns-2 simulation results in such a topology. The topology setup is such that each

node is 200 meters away from its closest neighbor. Figure 7a shows the plot for a cross communication pattern (similar to the one in Figure 6b). From the Figure we see that the model based computation predicts a higher throughput capacity than the one measured using ns-2. The reason is that the interference model in equation 25 is very tolerant to colliding channel assignments since it allows an accumulated interference of up to the signal strength of the sending node. In fact, $GreedyM$ as well as $RandomNode$ make the set $\mathcal{U}$ equal to $\mathcal{D}$. Despite the gap between measurements and prediction it is important to note the similar behavior of the estimate and the simulation results. And as we can see from Figure 7b, this also holds in the case of random communication. Here the $GreedyM$ and the $Randomnode_{12}$ estimate are closer together, a potential result of the randomness in communication. However, the estimates as well as the 802.11 measurements are still some gap away from the throughput capacity based on a conflict-free schedule (using 16 channels as mentioned earlier), as indicated by the dashed line in Figure 7b.

C. Random Topology

Contrary to chain and grid topologies, random topologies do not allow us to easily compute estimates based on conflict-free schedules. We consider random topologies of n nodes
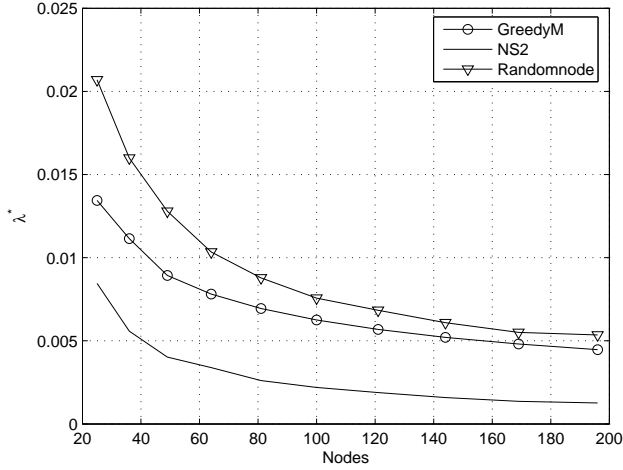
(a) Cross Traffic
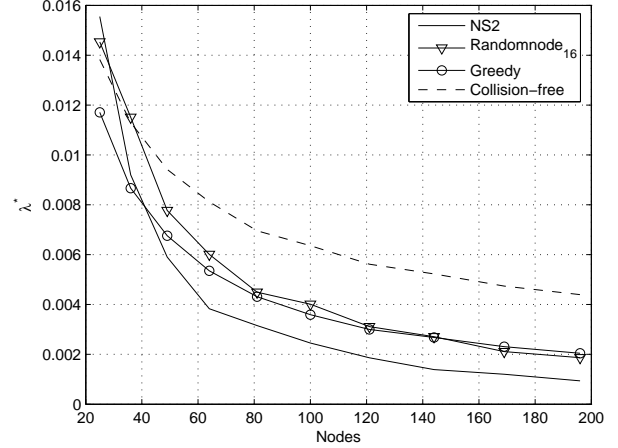
(b) Random Communication

Fig. 7. Grid Topology

distributed uniformly within an area of 1000×1000 meters. As in the previous topologies, all nodes have β_D configured such that the their transmission range equals 200m. Each node n_i acts as a traffic generator and has a random destination assigned, chosen uniformly out of $\mathcal{N} \backslash n_i$. Figure 8 shows the comparison between the estimate and the ns-2 simulation results. Obviously, both the estimate and the ns-2 measurements have a very similar behavior with regard on how the curves decay. However, despite this similarity, the estimate predicts a lower throughput capacity than the one measured by the 802.11 simulations. The reason might be that $GreedyM$ channel assignment with respect to random node topology and random communication is even less optimal than the schedule produced by the random access scheme 802.11. Compared to the grid, interfering nodes in a random topology typically are not located at the edge of the interference range, but spread around a certain mean. Or in other words, while in the grid the interference of a node n_B – located at half way between two nodes n_A and n_C – might be tolerated at both ends, the same node in a random topology is likely to be either closer to the one or the other side, disturbing at least one of the ongoing communications taking place in channel n_B^Γ. However, finding a good slot assignment algorithm which works for both the grid and the random topology, is not within the scope of this work, rather we provide a model that serves as a base for testing and verifying channel assignment strategies.

D. Discussion

The previous sections have illustrated the qualitative behavior of the model. In all the cases the throughput capacity λ^* showed a similar behavior – compared to the ns-2 simulation results – in terms of how the curves decay when the network becomes large. However, while for the chain and the grid the prediction was higher than the measured results, the opposite was observed in the case of random topologies. In fact, finding an optimal channel assignment ψ in random topologies is
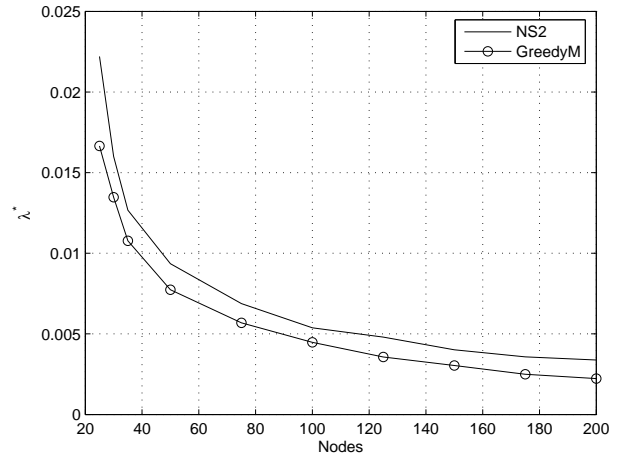

Fig. 8.   Random topology

a difficult problem. On the basis of the grid topology it was shown that a minimum channel assignment does not necessarily lead to a maximum throughput capacity. Rather, an optimal channel assignment goes hand in hand with the routing. From equation 19 we see that both the routing as well as the channel assignment directly affect the throughput capacity. Different routes $\Pi_{j,i}$ for communication pairs $(j, i) \in \Upsilon$ may result in different values of the random variable $B_{j,i}$. On the other hand, optimizing for $B_{j,i}$ may need too many channels. Clearly, there is a trade-off between routing and channel assignment and we can state that

$$\lambda_{max}^* = \max_{\substack{\eta \in \Theta \\ \psi \in \Psi}} \lambda^* \qquad (23)$$

for Θ being the class of all path assignments and Ψ the class of all possible channel assignments. Within this paper

we have looked at the channel assignment part only, assuming a shortest path routing η_s. One issue that might be of interest is whether maximizing throughput capacity involves shortest path routing or not, or formally:

$$\lambda^*_{max} \approx \max_{\psi \in \Psi} \ \lambda^*_{\eta_s}. \qquad (24)$$

VII. APPLYING THE MODEL

Besides the model serving as a basis for studying the maximum throughput capacity, it also facilitates the analysis of various network specific aspects with respect to throughput capacity. In this section we want to demonstrate this by means of two examples. The first example tackles the problem of finding the optimal transmission range in fixed-traffic networks. The second shows the effect of randomized signal propagation on throughput capacity under different interference models.

A. Optimal transmission range in fixed-traffic networks

Finding an optimal transmission range is commonly known as the connectivity problem, where we are interested in the minimum transmission range that leads to a connected network. Capacity can be studied in a similar way. Assume a fixed traffic density ξ, i.e., that every node transmits data with $\xi = W/K$ for some value K, where W is the maximum transmission rate. Such a traffic density can be modelled by dividing the common channel Γ into K subchannels $\Gamma^0, \Gamma^1, ...\Gamma^{K-1}$. Recall that nodes transmit data only within their assigned channel. And transmission is meant to be a node's own transmission as well as the forwarding load. The question now is at what transmission power (range) the nodes should transmit on average in order to maximize the throughput capacity. Figure 9 shows the throughput capacity as a function of transmission range for three different traffic densities. The network consists of 150 nodes uniformly distributed in an area of 1000×1000 square meters. From Figure 9 we see that the optimal transmission range changes with the traffic density. This is interesting since it stresses that, e.g., topology control should take into account the traffic density as well when looking for optimal transmission power selection. While it has been shown analytically that the maximum throughput capacity of a wireless multihop network is bound by the lowest transmission range R that makes the network connected [7], there is up to our knowledge no work on optimal transmission ranges for networks with a fixed traffic load. The model we propose in this paper supports such analysis, opening up the possibility of exploring in greater detail the relation between transmission range and traffic load within realistic network conditions.

B. Effect of randomized radio propagation

It is well known that representing the transmission range as a direct function of the distance does not reflect the reality of radio transmitters. In fact, the received transmission power can be seen as a random variable due to fading effects. The impact of randomized transmission power – also known as the effect of shadowing – has been analyzed with regard
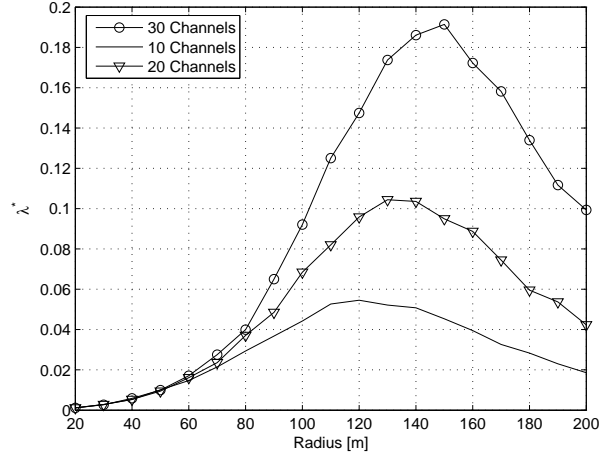
Fig. 9.   Optimal transmission range vs. network load

to network connectivity. It was shown that fading effects increase connectivity if the randomization itself is assumed to be symmetric for both ends of a potential link [4]. On the other hand if the fading effect is modelled as an independent random variable and communication is bi-directional, connectivity is observed to be degraded with increasing randomness [14]. Analyzing these effects with regard to throughput capacity is much more complex since it also influences the interference perceived while receiving data. As a benefit of our model, effects of signal propagation properties can be analyzed by just using an appropriate signal propagation function while computing the graph topology, as explained in section II. We have studied randomized radio propagation in two different interference models: the signal-to-noise interference model κ_{snr} as described in equation 8 and the so called protocol model $\kappa_{protocol}$ defined as

$$\kappa_{protocol}(p^r_{j,i}, \Lambda^a_i) = \begin{cases} 1 & \text{if } \Lambda^a_i < \beta_D \\ 0 & \text{otherwise.} \end{cases} \qquad (25)$$

The name *protocol* model refers to the notation used in [8] where the authors define a similar model. Obviously, the two models $kappa_{snr}$ and $\kappa_{protocol}$ are quite different in terms of interference-sensitivity. While κ_{snr} allows for interference up to a certain extent, $\kappa_{protocol}$ fails to receive correctly as soon as the perceived noise reaches the decoding threshold β_D. Figure 10 shows the effect of shadowing on throughput capacity under the two different interference models. The corresponding signal propagation model ϑ_{sh} is described in equation 1. For a given propagation distance d, the higher the standard deviation σ, the more the signal is spread around its mean. The nodes are supposed to be distributed within an area of 1000×1000 square meters. As we can see from Figure 10, in the case of a $\kappa_{protocol}$, the throughput capacity is highly affected by the randomized signal propagation while there is no big difference in the κ_{snr} model. One explanation might be that since the shadowing effect spreads the signals around a
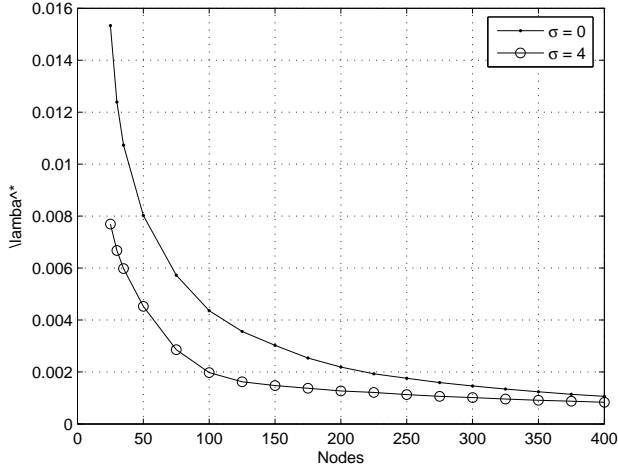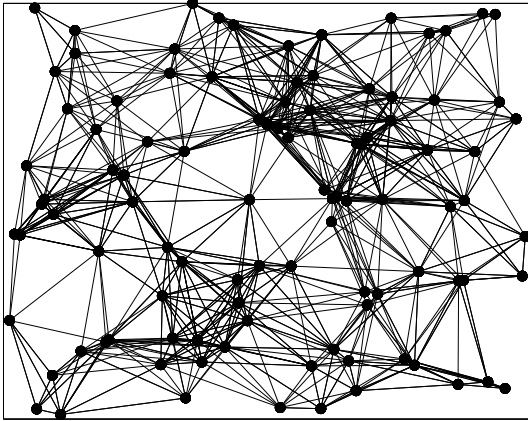
(a) $\kappa_{protocol}$
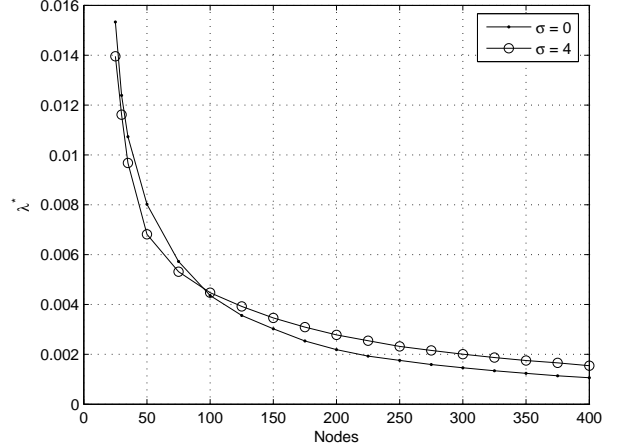
(b) κ_{snr}
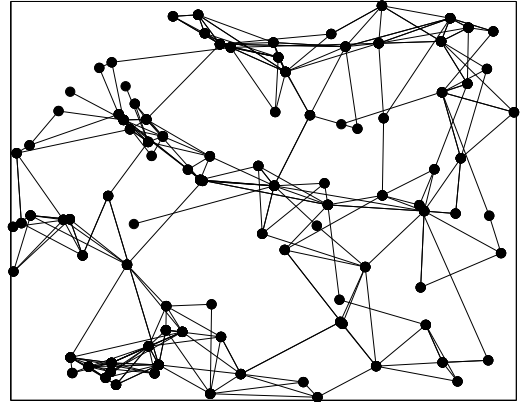
Fig. 10. Randomized radio propagation under different interference models

(a) Path loss radio propagation

(b) Randomized radio propagation

Fig. 11. The schedule graph

mean, the amplified parts significantly contribute to the noise while the other parts become negligible. And since $\kappa_{protocol}$ is much more sensitive to interference it also experiences a higher degradation in term of throughput capacity. The effect of shadowing is also illustrated in Figure 11 by means of the *schedule graph* for $N = 100$. As a result of randomized radio propagation the number of edges in the *schedule graph* is reduced. Therefore, links are shared by many communication pairs which leads to capacity degradation. However, as the network density becomes large, randomized radio propagation is observed to affect throughput capacity positively, especially in the case of κ_{snr} (Figure 10b) where effects of shadowing lead to an increase in throughput capacity. This again can be explained with the spreading effect caused by the randomization. If the network is very dense and the amount of

nodes within the average transmission range of a node is high, spreading the signal strength reduces the noise perceived at that node.

Interestingly, the node density at which the curves in Figure 10b cross, corresponds to the critical density needed to make two randomly chosen nodes connected with very high probability, as shown in Figure 12. Below the critical density of 100 nodes, two nodes may still be disconnected (in the case of randomized radio propagation); beyond the critical density, the probability P_{conn} of a path between two random nodes becomes almost 1. Therefore, we can subdivide the effect of randomized radio propagation as illustrated in Figure 10 into two parts, one that is caused by the lack of network connectivity (below 100 nodes), and one that results from an actual change in interference (beyond 100 nodes). In the
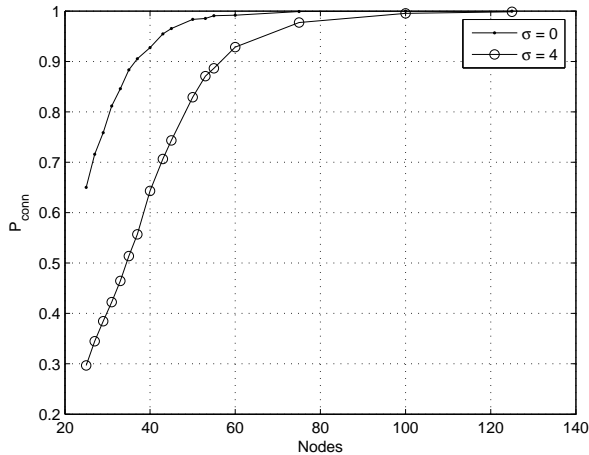
Fig. 12. Probability of two randomly chosen nodes to be connected

case of the *protocol* model $\kappa_{protocol}$, e.g., throughput capacity is degraded far beyond the critical node density. In the case of the *signal-to-noise* model, throughput capacity is increased beyond the critical node density. While effects of shadowing on throughput capacity have been analyzed for unidirectional links [16], there has up to our knowledge not been any work done so far under bidirectional, acknowledgement-based communication. As shown, the model we propose in this paper is a useful tool to explore this problem in greater detail.

VIII. CONCLUSIONS

Analyzing throughput capacity in Mobile Ad Hoc Networks (MANETs) is a challenging task that is of great practical importance. However, most approaches rely on simplified network models and either come up with asymptotic bounds or integer linear programming equations. In this paper we have developed a probabilistic model of throughput capacity as a random variable depending on node distribution, communication pattern, radio propagation and channel assignment. The model as proposed enables the study of throughput capacity under the effects of various network properties, but also serves as a basis for further research on the complex inter-action between routing and channel assignment with regard to throughput maximization. In the paper we compare model estimations with ns-2 simulation results and show how the model can be used to qualitatively predict throughput capacity of 802.11 ad hoc networks. One advantage of our approach lies in its decoupling from specific network characteristics, a feature that allows us to investigate throughput capacity under specific network topologies, communication patterns or signal propagation models. The paper illustrates this by means of two examples: optimal transmission ranges in fixed-traffic networks and effects of randomized radio propagation. In general it is shown that throughput capacity under the effect of shadowing is highly dependant on the interference model. For the particular case of a *signal-to-noise* interference model and bi-directional communication, throughput capacity was shown to increase with increasing randomization of the signals.

REFERENCES

[1] D. Aguayo, J. Bicket, S. Biswas, G. Judd, and R. Morris. Link-level measurements from an 802.11b mesh network. SIGCOMM, 2004.

[2] M. Andrews and L. Zhang. Routing and scheduling in multihop wireless networks with time-varying channels. In *SODA '04: Proceedings of the fifteenth annual ACM-SIAM symposium on Discrete algorithms*, pages 1031–1040, Philadelphia, PA, USA, 2004. Society for Industrial and Applied Mathematics.

[3] P. Barbrand and D. Yuan. Maximal throughput of spatial tdma in ad hoc networks. 3rd Scandinavian Workshop on Wireless Ad-hoc Networks, 2003.

[4] C. Bettstetter and C. Hartmann. Connectivity of wireless multihop networks in a shadow fading environment. In *MSWIM '03: Proceedings of the 6th ACM international workshop on Modeling analysis and simulation of wireless and mobile systems*, pages 28–32, New York, NY, USA, 2003. ACM Press.

[5] P. Bjorklund, P. Varbrand, and D. Yuan. Resource optimization of spatial tdma in ad hoc radio networks: A column generation approach. IEEE INFOCOM, March 2003.

[6] O. Dousse and P. Thiran. Connectivity vs capacity in dense ad hoc networks. IEEE INFOCOM, March 2004.

[7] J. Gomez and A. Campbell. A case for variable-range transmission power control in wireless ad hoc networks. IEEE INFOCOM, March 2004.

[8] P. Gupta and P.R.Kumar. The capacity of wireless networks. *IEEE Trans. On Information Theory*, 46(2), March 2000.

[9] S. Krumke and M. Marathe. Models and approximation algorithms for channel assignment in radio networks. *Wirel. Netw.*, 7(6):575–584, 2001.

[10] J. Li, C. Blake, D. S. D. Couto, H. I. Lee, and R. Morris. Capacity of ad hoc wireless networks. In *MobiCom '01: Proceedings of the 7th annual international conference on Mobile computing and networking*, pages 61–69, New York, NY, USA, 2001. ACM Press.

[11] S. Ramanathan and E. L. Lloyd. Scheduling algorithms for multihop radio networks. *IEEE/ACM Trans. Netw.*, 1(2):166–177, 1993.

[12] T. S. Rappaport. *Wireless communications, principles and practice.* Prentice Hall, 1996.

[13] M. Sanchez, J. Zander, and T. Giles. Combined routing and scheduling for spatial tdma in multihop ad hoc networks. 5th International Symposium on Wireless Personal Multimedia Communications, 2002.

[14] P. Stuedi and G. Alonso. Connectivity in the presence of shadowing in 802.11 ad hoc networks. IEEE Wireless and Communications and Networking Conference (WCNC), 2005.

[15] The VINT Project. The NS network simulator, 2002.

[16] S. Toumpis and A. Goldsmith. Capacity regions for wireless adhoc networks, 2001.

[17] G. Zhou, T. He, S. Krishnamurthy, and J. Stankovic. Impact of radio irregularity on wireless sensor networks. *MobiSys*, 2004.

[18] M. Zorzi and S. Pupolin. Optimum transmission ranges in multihop packet radio networks in the presence of fading. *IEEE Trans. On Communication*, 43(7), July 1995.